

Angle-dependent x-ray absorption spectroscopy study of Zn-doped GaN

J. W. Chiou, S. Mookerjee,^{a)} K. V. R. Rao,^{b)} J. C. Jan, H. M. Tsai, K. Asokan,^{a)}
W. F. Pong,^{c)} and F. Z. Chien

Department of Physics, Tamkang University, Tamsui, Taiwan 251, Republic of China

M.-H. Tsai

Department of Physics, National Sun Yat-Sen University, Kaohsiung, Taiwan 804, Republic of China

Y. K. Chang and Y. Y. Chen

Institute of Physics, Academia Sinica, Taipei, Taiwan 107, Republic of China

J. F. Lee

Synchrotron Radiation Research Center, Hsinchu, Taiwan 300, Republic of China

C. C. Lee and G. C. Chi

Optical Science Center, National Central University, Chung-Li, Taiwan 320, Republic of China

(Received 1 July 2002; accepted 11 September 2002)

As-grown and Zn-implanted wurtzite GaN samples have been studied by angle-dependent x-ray absorption near edge structure (XANES) measurements at the N and Ga *K*-edges and the Ga *L*₃-edge. The angle dependence of the XANES spectra shows that the Ga–N bonds lying in the bilayer have lower energies than bonds along the *c*-axis, which can be attributed to the polar nature of the GaN film. The comparison of the Ga *L*₃-edge XANES spectra of as-grown and Zn-doped GaN reveals significant dopant induced enhancement of near-edge Ga *d*-derived states. © 2002 American Institute of Physics. [DOI: 10.1063/1.1518776]

The potential of group III nitrides in the development of such devices as short-wavelength lasers, blue and ultraviolet light emitting diodes, high-temperature and high-power electronics, and magneto-electronic devices is now well established.^{1–3} The successful fabrication of *p*-type GaN using Mg as dopant accelerated the development of GaN-based devices.⁴ Recent studies of Mg-doped GaN provide an insight into the doping processes in this system.^{5–9} For example, incorporation of Mg has been known to increase the defect concentration and induce the appearance of a mixture of crystal phases in the material.⁶ Introducing hydrogen during the growth and doping process was found to compensate Mg acceptors^{5,7} through formation of a Mg–H complex.⁸ A self-compensation mechanism involving N vacancies has also been proposed to explain the dependence of hole density on the dopant concentration.⁹ In comparison, the properties of other group II dopants like Zn are less well understood. Doping with only Zn was observed to lead to the formation of highly resistive material, while codoping with Mg produced a low resistive *p*-type GaN layer.¹⁰ A moderate amount of Zn dopant appears to reduce the defect concentration in GaN. To better understand the properties of GaN on incorporation of Zn dopants, we have performed angle-dependent x-ray absorption near edge structure (XANES) measurements at the N and Ga *K*-edges and the Ga *L*₃-edge for as-grown and Zn implanted GaN.

X-ray absorption spectra were recorded using the facilities at the Synchrotron Radiation Research Center (SRRC) at Hsinchu, Taiwan. For all samples, the N *K*-edge and Ga

*L*₃-edge spectra were obtained using the high-energy spherical grating monochromator beamline in a vacuum better than 10^{−9} Torr, by the fluorescence yield method. Ga *K*-edge spectra were obtained using the wiggler 17C beamline. The direction of the electric polarization vector was varied with respect to the orientation of the thin film specimen, and spectra were recorded for angles from 10° to 70° or 80° between the incident photon direction and the surface normal of the film. The GaN samples were grown by metal–oxide chemical vapor deposition on a sapphire substrate up to approximately 1400 Å followed by annealing for 5 min at 1100 °C. The Zn-doped sample was obtained by implanting 200 KeV Zn ions at a dose of 5 × 10¹⁴ cm^{−2}. A capping layer of Zn was deposited to retard the decomposition of GaN during annealing. The GaN samples were characterized by photoluminescence (PL), x-ray diffraction (XRD), and electrical measurements. Details of the growth process and characterization results are reported elsewhere.¹¹

Figure 1(a) shows PL spectra at 25 K of the as-grown and Zn-doped GaN samples. The prominent feature at 3.45 eV in the spectrum of the as-grown GaN sample has been designated as (D⁰, X).¹² The weak features at ~3.27 eV correspond to the (D⁰-A⁰) peak. The spectrum of the Zn-doped GaN sample has a strong broad peak centered at 2.9 eV. This broad peak has been called the A-band, and was attributed to the Zn complex or Zn_{Ga}.^{13,14} Bands associated with Zn_N[−], Zn_N^{2−} and Zn_N[−] were reported earlier at 2.6, 2.2, and 1.8 eV, respectively,¹⁴ for higher concentrations of Zn are absent in the spectrum of the implanted sample shown in Fig. 1(a). The XRD patterns for both as-grown and Zn-doped GaN samples as shown in Fig. 1(b) have a predominant reflection of (002) at around 35°, which is consistent with the hexagonal (wurtzite) structure of the specimens. The pattern of the GaN powder specimen, which has a mixed phase of cubic and hexagonal symmetry, is also shown for comparison. Our

^{a)}Permanent address: Department of Physics, University of Rajasthan, Jaipur 302 004, India.

^{b)}On leave from: Nuclear Science Center, Aruna Asaf Ali Marg, New Delhi 110 067, India.

^{c)}Author to whom correspondence should be addressed; electronic mail: wfpong@mail.tku.edu.tw

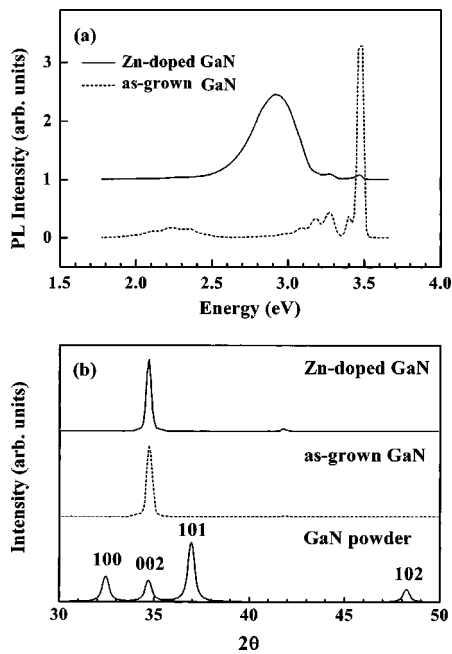


FIG. 1. (a) PL spectra at 25 K for as-grown GaN (dashed line) and Zn-doped GaN (solid line) samples. (b) X-ray diffraction pattern for as-grown GaN, Zn-doped GaN, and powder GaN samples.

XRD characterization shows that the Zn implanted samples do not have a mixed phase.

Figures 2 and 3 show the XANES spectra of as-grown and Zn-doped GaN samples at the N and Ga *K*-edges, respectively. The upper inset in Fig. 2 shows the incident angle θ relative to the *c*-axis. The dependence of the peak intensity on the incident angle for the N *K*-edge (Fig. 2) has been regarded as an evidence of anisotropy in the *p* states and an indicator of the wurtzite crystal phase in GaN;¹⁵ the similarity of the spectra for the as-grown and the Zn-doped samples indicates the retention of the wurtzite structure upon doping in consistency with our XRD result. An implantation-induced

broadening of the XANES feature and the appearance of a pre-edge feature were reported in GaN implanted with N and O ions.¹⁶ This finding was attributed to lattice damage on implantation and to vacancies and interstitial. Figures 2 and 3 show that implantation did not alter the absorption edge. The absence of a pre-edge structure or any additional broadening of the XANES resonance indicates that post-implantation annealing could reduce implantation-induced lattice damage and defects.

The orientation dependence of the *K*-edge spectra for the as-grown and Zn-doped samples may provide a pointer to changes in the electronic property as a result of Zn implantation. For GaN films grown on sapphire, the surface is perpendicular to the *c*-axis. For each atom, there are three Ga–N bonds lying in the bilayer, which may be called bilayer bonds (σ bond in Ref. 17), and one Ga–N bond along the *c*-axis, which may be called the *c*-axis bond (π bond in Ref. 17). The bilayer- and *c*-axis-bond states are preferentially probed at small and large incidence angles, respectively. This is because the polarization of photons is parallel with the bilayer and *c*-axis bonds at small and large incident angles, respectively.

The variations in peak positions with the photon incident angle are similar for both as-grown and Zn-doped GaN samples and for both the N and Ga *K*-edge spectra, which are similar to previous observations for undoped GaN.^{15,17} Further, for the Ga *K*-edge spectra (Fig. 3), a ~ 2 eV difference in the position of the dominant peak between the bilayer (σ) and *c*-axis (π) spectra observed earlier for undoped GaN¹⁷ is also seen for both the as-grown and Zn-implanted spectra. The small difference between the *c*-axis and bilayer bond lengths is unlikely to be the origin of this shift. Wurtzite GaN has lattice constants of $a=3.190$ Å and $c=5.189$ Å. The c/a ratio of 1.627 is slightly smaller than the ideal ratio of $2\sqrt{2}/\sqrt{3}=1.633$ by 0.4%. Since a is larger than 1.633 times the Ga–N bond length of 1.95 Å by about 0.2%,

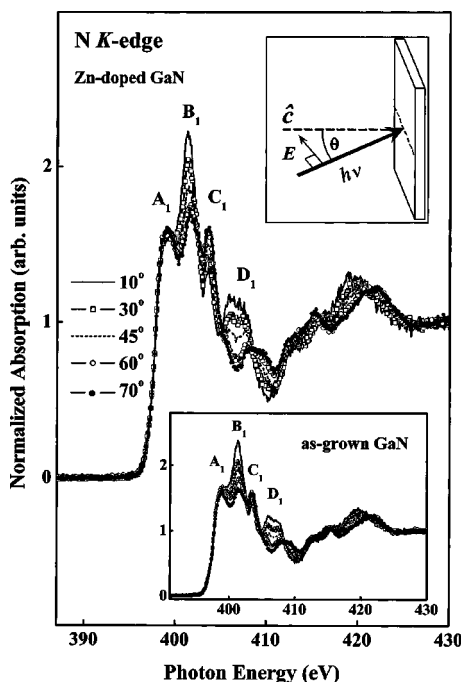


FIG. 2. Dependence of the N *K*-edge XANES spectra on the photon incident angle for Zn-doped GaN. The upper inset defines the photon incident angle. The lower inset shows the corresponding as-grown GaN spectra.

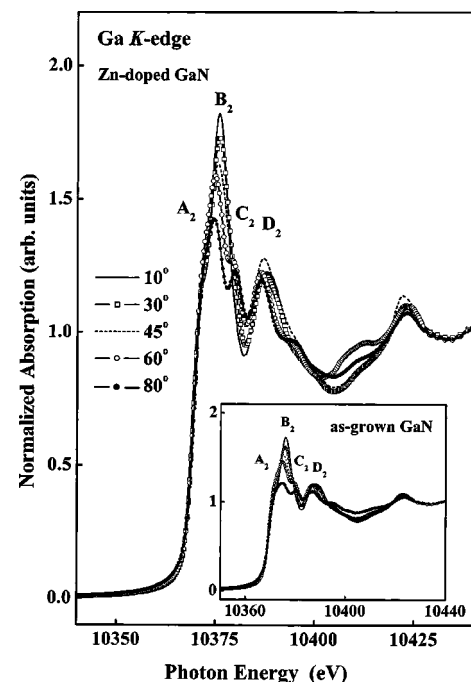


FIG. 3. Dependence of the Ga *K*-edge XANES spectra on the incident angle for Zn-doped GaN. The lower inset shows the corresponding as-grown GaN spectra.

the c/a ratio of 1.627 implies that the c -axis-bond length is only slightly smaller than the bi-layer-bond length by about 0.01 Å. The difference between the electronic properties of the bilayer and c -axis bonds may arise from the electric-dipole-layer array along the c -axis. GaN is a relatively ionic material. Ga and N ions have substantial effective charges. Along the c -axis each Ga–N bilayer is a dipole layer. Thus, the GaN film forms an array of dipole layers, which gives rise to a polarization field.¹⁸ Either for an N-terminated GaN(0001) or a Ga-terminated GaN(0001) film, the polarization field pushes the c -axis-bond electronic charge towards the negative N ion, which raises the energies of c -axis-bond states. This effect is much smaller and in opposite direction for bilayer-bond states because these bonds have a large angle from the c -axis. Thus, the observed asymmetric electronic property between c -axis- and bilayer-bond states is likely to be due to the polar nature of the film.

The anisotropy arising from this asymmetry of electronic properties is illustrated by the angle dependence of the spectra in Figs. 2 and 3. At the N K -edge (Fig. 2), features A_1 to D_1 can be correlated with the four features in the calculated N derived p partial density of state (PDOS).¹⁷ The spectra for $\theta=10^\circ$ and $\theta=70^\circ$, shown in Fig. 2, agree well, respectively, with the σ bond (bilayer bond) and π bond (c -axis bond) XANES spectra for undoped GaN.¹⁷ Variations of the intensities of features A_1 to D_1 from $\theta=10^\circ$ to $\theta=70^\circ$ are consistent with a shift of the bilayer-bond spectrum continuously to the higher energy c -axis-bond spectrum described in the previous paragraph. The Ga K -edge spectra (Fig. 3) are similar to those of undoped GaN observed previously.^{3,17} Figure 3 shows that the weight of the spectrum shifts to higher energies from $\theta=10^\circ$ to $\theta=80^\circ$, which is consistent with the N K -edge results, showing that the c -axis bond states have higher energies than the bilayer bond states.

Figure 4 shows the Ga L_3 -edge XANES spectra of Zn-doped and as-grown GaN. The inset in Fig. 4 shows that the spectrum of the as-grown GaN is insensitive to the photon incident angle, which suggests that the states contributing to the spectrum are dominantly s -like in agreement with previous observations.^{17,19} Since Ga L_3 -edge XANES measures unoccupied s and d derived states, this result shows that the conduction band near conduction band minimum does not contain significant Ga d -orbital contribution. This is because the Ga $3d$ band is well below Fermi energy or valence band maximum. In contrast, the Ga L_3 -edge XANES spectra of Zn-doped GaN show significant dependence on the photon incident angle, which suggests that Zn dopants induce significant near-edge d -like states. An alternative explanation is that Zn dopants induce asymmetry in the crystal field or enhance the Ga–N coupling, which lowers energies of some higher-energy Ga d orbitals, so that they contribute to the near-edge Ga L_3 -edge spectra in addition to the s -orbital contribution and enhance features A_3 and B_3 , as shown in Fig. 4.

In conclusion, the angle-dependent XANES measurements at the N and Ga K -edges and the Ga L_3 -edge show that the Ga–N bonds lying in the bilayer have lower energies than those lying along the c -axis. The Ga L_3 -edge XANES spectra indicate significant Zn-dopant induced enhancement of near-edge Ga d -derived states.

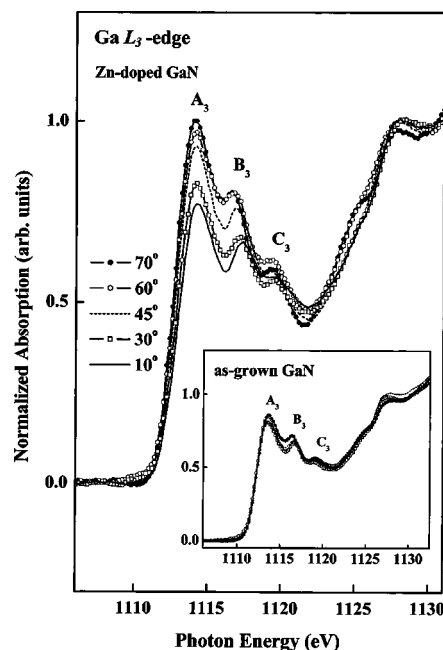


FIG. 4. Dependence of the Ga L_3 -edge XANES spectra on the incident angle for Zn-doped GaN. The lower inset shows the corresponding as-grown GaN spectra. The spectral features B_3 and C_3 in the Zn-doped GaN spectra shift to higher energies with decreasing incident angle.

This work was supported by the National Science Council of the Republic of China under Contract No. NSC-90-2112-M-032-019.

- ¹S. Nakamura, T. Mukai, and M. Senoh, *J. Appl. Phys.* **76**, 8189 (1994).
- ²S. Nakamura, M. Senoh, N. Iwasa, and S. Nagahama, *Jpn. J. Appl. Phys., Part 2* **34**, L797 (1995).
- ³S. Nakamura, M. Senoh, N. Iwasa, S. Nagahama, T. Yamada, T. Matsushita, Y. Sugimoto, and H. Kiyoku, *Appl. Phys. Lett.* **70**, 868 (1997).
- ⁴H. Amano, M. Kito, K. Hiramatsu, and I. Akasaki, *Jpn. J. Appl. Phys., Part 2* **28**, L2112 (1989).
- ⁵W. Gotz, N. M. Johnson, D. P. Bour, M. D. McCluskey, and E. E. Haller, *Appl. Phys. Lett.* **69**, 3725 (1996).
- ⁶Y. C. Pan, S. F. Wang, W. H. Lee, M. C. Lee, W. K. Chen, W. H. Chen, L. Y. Jang, J. F. Lee, C. I. Chiang, H. Chang, K. T. Wu, and D. S. Lin, *Appl. Phys. Lett.* **78**, 31 (2001).
- ⁷J. Neugebauer and C. G. Van de Walle, *Appl. Phys. Lett.* **68**, 1829 (1996).
- ⁸S. Limpijumnong, J. E. Northrup, and Chris G. Van de Walle, *Phys. Rev. Lett.* **87**, 205505 (2001).
- ⁹U. Kaufmann, P. Schlotter, H. Obloh, K. Kohler, and M. Maier, *Phys. Rev. B* **62**, 10867 (2000).
- ¹⁰K. S. Kim, M. S. Han, G. M. Yang, C. J. Youn, H. J. Lee, H. K. Cho, and J. Y. Lee, *Appl. Phys. Lett.* **77**, 1123 (2000).
- ¹¹C. C. Lee and G. C. Chi (private communication).
- ¹²B. J. Skromme and G. L. Martinez, *MRS Internet J. Nitride Semicond. Res.* **5S1**, W9.8 (2000).
- ¹³P. Bergman, Gao Ying, B. Monemar, and P. O. Holtz, *J. Appl. Phys.* **61**, 4589 (1987).
- ¹⁴B. Monemar, O. Lagerstedt, and H. P. Gislason, *J. Appl. Phys.* **51**, 625 (1980).
- ¹⁵M. Katsikini, E. C. Paloura, and T. D. Moustakas, *Appl. Phys. Lett.* **69**, 4206 (1996); M. Katsikini, E. C. Paloura, and T. D. Moustakas, *J. Appl. Phys.* **83**, 1437 (1998).
- ¹⁶M. Katsikini, E. C. Paloura, J. Bollmann, E. Holub-Krappe, and W. T. Masselink, *J. Electron Spectrosc. Relat. Phenom.* **101–103**, 689 (1999).
- ¹⁷K. Lawniczak-Jablonska, T. Suski, I. Gorczyca, N. E. Christensen, K. E. Attenkofer, R. C. C. Perera, E. M. Gullikson, J. H. Underwood, D. L. Ederer, and Z. Lilienthal-Weber, *Phys. Rev. B* **61**, 16623 (2000).
- ¹⁸M.-H. Tsai, O. F. Sankey, K. E. Schmidt, and I. S. T. Tsong, *Mater. Sci. Eng., B* **88**, 40 (2002).
- ¹⁹C. B. Stagarescu, L.-C. Duda, K. E. Smith, J. H. Guo, J. Nordgren, R. Singh, and T. D. Moustakas, *Phys. Rev. B* **54**, R17335 (1996).